

Hydroxyphosphine Ligand for Nickel-Catalyzed Cross-Coupling through Nickel/Magnesium Bimetallic Cooperation

Naohiko Yoshikai, Hirokazu Matsuda, and Eiichi Nakamura*

Department of Chemistry, The University of Tokyo, Bunkyo-ku, Tokyo 113-0033, Japan

Received April 17, 2009; E-mail: nakamura@chem.s.u-tokyo.ac.jp

Abstract: We report here that hydroxyphosphine ligands (PO ligands) significantly accelerate nickel-catalyzed cross-coupling reactions of nickel–PO–Grignard unreactive aryl electrophiles and Grignard reagents. The new catalytic system based on the nickel–PO–Grignard combination allows facile activation of unreactive aryl halides such as fluorides, chlorides, polyfluorides, and polychlorides as well as phenol derivatives such as carbamates and phosphates to give the corresponding cross-coupling products in good to excellent yields. We ascribe the high catalytic activity to a nickel phosphine/magnesium alkoxide bimetallic species that forms from the nickel precatalyst, the PO ligand, and the Grignard reagent and undergoes activation of the aryl–X bond by a cooperative push–pull action of the nucleophilic nickel and Lewis acidic magnesium centers. This mechanistic conjecture was corroborated by kinetic isotope effect experiments and density functional theory calculations. Being distinct from the conventional three-centered mechanism for oxidative addition, the proposed mechanism for the C–X bond activation offers a new concept for the design of cross-coupling reactions as well as other homogeneous catalyses involving activation of electrophilic substrates.

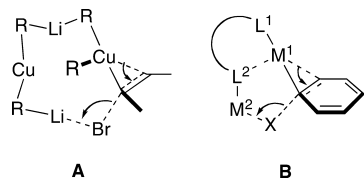
Introduction

Since the initial report of nickel-catalyzed cross coupling of a Grignard reagent with an sp^2 halide by Kumada/Tamao and Corriu (KTC),¹ the group-10 metal-catalyzed cross-coupling reaction of an aryl or alkenyl electrophile and an organometallic reagent has been established as a versatile synthetic method for the formation of C(sp^2)–C bonds as the result of the development of such variants as the Negishi,² Migita–Kosugi–Stille,³ and Suzuki–Miyaura⁴ coupling reactions.⁵ In addition to the conventional electrophiles, such as aryl iodides, bromides, and triflates, rather unreactive aryl chlorides,⁶ fluorides,^{7,8} and phenol

derivatives can be used as coupling partners,^{9–14} but these necessitate a careful choice of the catalyst because of the sluggishness of the oxidative addition step, the first step of the catalytic cycle. A common technology for bringing these

- (1) (a) Tamao, K.; Sumitani, K.; Kumada, M. *J. Am. Chem. Soc.* **1972**, *94*, 4374–4376. (b) Corriu, R. J. P.; Masse, J. P. *J. Chem. Soc., Chem. Commun.* **1972**, 144a.
- (2) Negishi, E.-i. *Acc. Chem. Res.* **1982**, *15*, 340–348.
- (3) (a) Stille, J. K. *Angew. Chem., Int. Ed. Engl.* **1986**, *25*, 508–523. (b) Farina, V.; Krishnamurthy, V.; Scott, W. J. *Org. React.* **1997**, *50*, 1–652.
- (4) (a) Miyaura, N.; Suzuki, A. *Chem. Rev.* **1995**, *95*, 2457–2483. (b) Suzuki, A. *J. Organomet. Chem.* **2002**, *653*, 83–90.
- (5) (a) *Metal-catalyzed Cross-coupling Reactions*, 2nd ed.; de Meijere, A., Diederich, F., Eds.; Wiley-VCH: New York, 2004. (b) *Cross-Coupling Reactions: A Practical Guide*; Miyaura, N., Ed.; Springer: Berlin, 2002.
- (6) Littke, A. F.; Fu, G. C. *Angew. Chem., Int. Ed.* **2002**, *41*, 4176–4211.
- (7) (a) Kiso, Y.; Tamao, K.; Kumada, M. *J. Organomet. Chem.* **1973**, *50*, C12–C14. (b) Böhm, V. P. W.; Gstöttmayr, C. W. K.; Weskamp, T.; Herrmann, W. A. *Angew. Chem., Int. Ed.* **2001**, *40*, 3387–3389. (c) Mongin, F.; Mojovic, B.; Guillaumet, B.; Trécourt, F.; Quéguiner, G. *J. Org. Chem.* **2002**, *67*, 8991–8994. (d) Dankwardt, J. W. *J. Organomet. Chem.* **2005**, *690*, 932–938. (e) Saeki, T.; Takashima, Y.; Tamao, K. *Synlett* **2005**, 1771–1774. (f) Ackermann, L.; Born, R.; Spatz, J. H.; Meyer, D. *Angew. Chem., Int. Ed.* **2005**, *44*, 7216–7219. (g) Inamoto, K.; Kuroda, J.; Sakamoto, T.; Hiroya, K. *Synthesis* **2007**, 2853–2861.

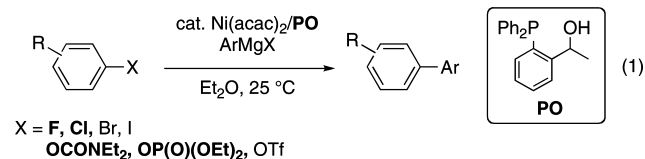
- (8) Schaub, T.; Backes, M.; Radius, U. *J. Am. Chem. Soc.* **2006**, *128*, 15964–15965.
- (9) (a) Zim, D.; Lando, V. R.; Dupont, J.; Monteiro, A. L. *Org. Lett.* **2001**, *3*, 3049–3051. (b) Roy, A. H.; Hartwig, J. F. *J. Am. Chem. Soc.* **2003**, *125*, 8704–8705. (c) Nguyen, H. N.; Huang, X.; Buchwald, S. L. *J. Am. Chem. Soc.* **2003**, *125*, 11818–11819. (d) Tang, Z.-Y.; Hu, Q.-S. *J. Am. Chem. Soc.* **2004**, *126*, 3058–3059. (e) Limmert, M. E.; Roy, A. H.; Hartwig, J. F. *J. Org. Chem.* **2005**, *70*, 9364–9370. (f) Ackermann, L.; Althammer, A. *Org. Lett.* **2006**, *8*, 3457–3460. (g) Zhang, L.; Meng, T.; Wu, J. *J. Org. Chem.* **2007**, *72*, 9346–9349. (h) Wu, J.; Zhang, L.; Xia, H. G. *Tetrahedron Lett.* **2006**, *47*, 1525–1528. (i) Tang, Z.-Y.; Spinella, S.; Hu, Q.-S. *Tetrahedron Lett.* **2006**, *47*, 2427–2430.
- (10) (a) Percec, V.; Bae, J.-Y.; Hill, D. H. *J. Org. Chem.* **1995**, *60*, 1060–1065. (b) Percec, V.; Golding, G. M.; Smidkral, J.; Weichold, O. *J. Org. Chem.* **2004**, *69*, 3447–3452.
- (11) Sengupta, S.; Leite, M.; Raslan, D. S.; Quesnelle, C.; Snieckus, V. *J. Org. Chem.* **1992**, *57*, 4066–4068.
- (12) Hayashi, T.; Katsuro, Y.; Okamoto, Y.; Kumada, M. *Tetrahedron Lett.* **1981**, *22*, 4449–4452.
- (13) (a) Quasdorf, K. W.; Tian, X.; Garg, N. K. *J. Am. Chem. Soc.* **2008**, *130*, 14422–14423. (b) Guan, B.-T.; Wang, Y.; Li, B.-J.; Yu, D.-G.; Shi, Z.-J. *J. Am. Chem. Soc.* **2008**, *130*, 14468–14470. (c) Li, B.-J.; Li, Y.-Z.; Lu, X.-Y.; Liu, J.; Guan, B.-T.; Shi, Z.-J. *Angew. Chem., Int. Ed.* **2008**, *47*, 10124–10127.
- (14) (a) Wenkert, E.; Michelotti, E. L.; Swindell, C. S. *J. Am. Chem. Soc.* **1979**, *101*, 2246–2247. (b) Wenkert, E.; Michelotti, E. L.; Swindell, C. S.; Tingoli, M. *J. Org. Chem.* **1984**, *49*, 4894–4899. (c) Dankwardt, J. W. *Angew. Chem., Int. Ed.* **2004**, *43*, 2428–2432. (d) Guan, B.-T.; Xiang, S.-K.; Wang, B.-Q.; Sun, Z.-P.; Wang, Y.; Zhao, K.-Q.; Shi, Z.-J. *J. Am. Chem. Soc.* **2008**, *130*, 3268–3269. (e) Tobisu, M.; Shimasaki, T.; Chatani, N. *Angew. Chem., Int. Ed.* **2008**, *47*, 4866–4869. (f) Guan, B.-T.; Xiang, S.-K.; Wu, T.; Sun, Z.-P.; Wang, B.-Q.; Zhao, K.-Q.; Shi, Z.-J. *Chem. Commun.* **2008**, 1437–1439.

Chart 1. Possible Modes of C(sp²)-X Bond Oxidative Addition

unreactive electrophiles into the cycle has been the use of catalysts bearing a bulky, electron-rich phosphine ligand or a bulky N-heterocyclic carbene (NHC),⁶ which facilitates the formation of a coordinatively unsaturated, highly nucleophilic catalytic species.

In this article, we present a new push-pull design of the ligand to promote the cross-coupling reaction. The central hypothesis is the synergistic use of a group-10 nucleophilic metal and a Lewis acidic main-group metal for promotion of carbon-halogen or carbon-pseudohalogen bond cleavage. The hypothesis originates from our previous mechanistic study of the oxidative addition reaction of a lithium diorganocuprate(I) with an alkenyl bromide,^{15–17} where the theory and experiments indicated that the d¹⁰ Cu(I) atom and the Li(I) cation act synergistically to activate the C-Br bond in a push-pull transition state (TS) **A** (Chart 1). We therefore envisioned that a similar synergistic scenario **B** may be orchestrated for d¹⁰ metals such as Ni(0) and Pd(0) through the design of a bidentate ligand L¹-L² that can simultaneously coordinate to a group-10 metal (M¹) and a Lewis acidic metal (M²).

This hypothesis led us to find that ligand **PO** and related hydroxyphosphine ligands (**PO** ligands) promote the nickel-catalyzed KTC reaction (eq 1):



The ligand is neither sterically demanding nor electron-rich yet significantly accelerates and promotes the cross-coupling of Grignard reagents with aryl fluorides, chlorides, polyfluorides, and polychlorides.¹⁸ The catalytic system also shows a high reactivity toward less reactive phenol derivatives such as carbamates and phosphates. Experimental and theoretical analyses have revealed that the turnover-limiting step of this reaction is different from that of the conventional KTC reaction using a nickel-bisphosphine catalyst¹⁹ and that upon deprotonation by the Grignard reagent, **PO** organizes the nucleophilic Ni(0) atom and the Lewis acidic Mg(II) ion to synergistically promote the C-X bond cleavage (see **B** in Chart 1: L¹ = Ph₂P; L² = O⁻; M¹ = Ni; M² = Mg). The ability of related **PO** ligands to control transition-metal-catalyzed reactions of organometallic reagents has also recently been demonstrated for asymmetric copper-catalyzed C-C bond-formation reactions. Thus, the chiral

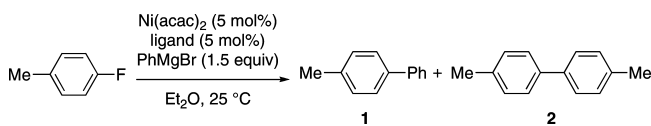
(15) Nakamura, E.; Mori, S. *Angew. Chem., Int. Ed.* **2000**, *39*, 3750–3771.

(16) Yoshikai, N.; Nakamura, E. *J. Am. Chem. Soc.* **2004**, *126*, 12264–12265.

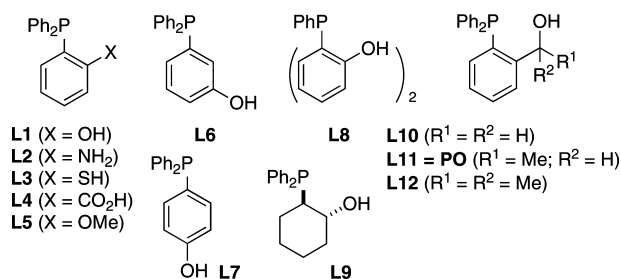
(17) Yoshikai, N.; Iida, R.; Nakamura, E. *Adv. Synth. Catal.* **2008**, *350*, 1063–1072.

(18) Preliminary communication: Yoshikai, N.; Mashima, H.; Nakamura, E. *J. Am. Chem. Soc.* **2005**, *127*, 17978–17979.

(19) Yoshikai, N.; Matsuda, H.; Nakamura, E. *J. Am. Chem. Soc.* **2008**, *130*, 15258–15259.

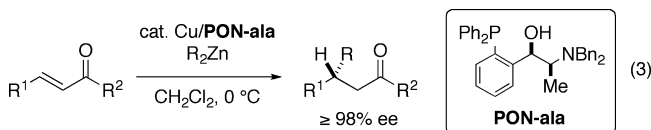
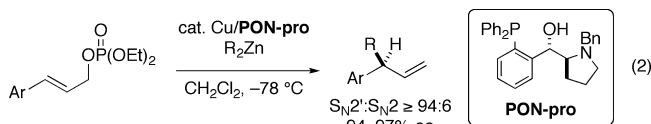
Table 1. Screening of Ligands for Ni-Catalyzed Cross-Coupling of 4-Fluorotoluene and Phenylmagnesium Bromide

entry	ligand	time (h)	yield (%) ^a	
			1	2
1	PPh ₃	15	5	0
2	L1	0.5	65	10
3	L2	0.5	38	0
4	L3	0.5	0	0
5	L4	0.5	4	0
6	L5	15	11	0
7	L6	15	5	0
8	L7	15	3	0
9	L8	0.5	7	0
10	L9	0.5	50	<1
11	L10	0.5	75	1
12	L11	0.5	94	0
13	L12	0.5	2	0
14 ^b	L11	1	94 ^c	0
15 ^d	L11	0.5	38	0



^a Determined by GC using *n*-tridecane as an internal standard. ^b The reaction was carried out using 1 mol % Ni(acac)₂, 1 mol %, **L11**, and 1.1 equiv of PhMgBr. ^c Isolated yield. ^d The reaction was carried out in THF.

aminohydroxyphosphine ligands (**PON** ligands) **PON-pro** and **PON-ala** promote highly enantioselective copper-catalyzed allylic substitution and conjugate addition reactions of organozinc reagents, respectively (eqs 2 and 3).²⁰

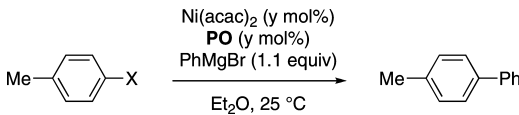


The deprotonated form of the **PON** ligand has been considered to serve as a scaffold for both the nucleophilic Cu(I) and Lewis acidic Zn(II) ions to achieve push-pull activation of the electrophile in a highly stereoselective manner (see below).

Results and Discussion

Ligand Screening. We examined the 12 ligands **L1–L12** listed in Table 1 for the nickel-catalyzed KTC reaction and found

(20) (a) Yoshikai, N.; Miura, K.; Nakamura, E. *Adv. Synth. Catal.* **2009**, *351*, 1014–018. (b) Hajra, A.; Yoshikai, N.; Nakamura, E. *Org. Lett.* **2006**, *8*, 4153–4155.

Table 2. Ni/PO-Catalyzed Cross-Coupling of *p*-Tolyl Halide or Pseudohalide and Phenylmagnesium Bromide


entry	X	y	time (h)	yield (%) ^a
1	F	1	1	94 ^b
2	Cl	1	1/3	97
3	Br	0.2	3	91
4	I	0.05	2	98
5	OTf	1	2	95
6	SMe	1	1	5
7	SMe	5	24	62

^a Determined by GC using *n*-tridecane as an internal standard. ^b Isolated yield.

an intriguing structure–reactivity relationship. The cross-coupling reaction of 4-fluorotoluene and phenylmagnesium bromide in Et₂O at 25 °C in the presence of a nickel precatalyst consisting of 5 mol % Ni(acac)₂ (acac = acetylacetonato) and 5 mol % ligand afforded the data summarized in Table 1. While the standard triphenylphosphine ligand was ineffective, producing the cross-coupling product (4-methylbiphenyl, **1**) in only 5% yield after 15 h (entry 1), triphenylphosphines bearing acidic ortho substituents (OH, NH₂, SH, CO₂H in **L1**–**L4**, respectively) showed some acceleration effects. Thus, the phenolic ligand **L1** gave **1** in 65% yield accompanied by a small amount (10%) of a homocoupling product (4,4'-dimethylbiphenyl, **2**) after 30 min (entry 2). The aniline ligand **L2** also showed a moderate acceleration effect, affording **1** in 38% yield (entry 3). On the other hand, thiol- and carboxylic acid derivatives (**L3** and **L4**) were ineffective (entries 4 and 5). The anisole ligand **L5** was less effective than **L1** (11% yield of **1** after 15 h; entry 6), indicating the importance of the free hydroxy group in **L1**.

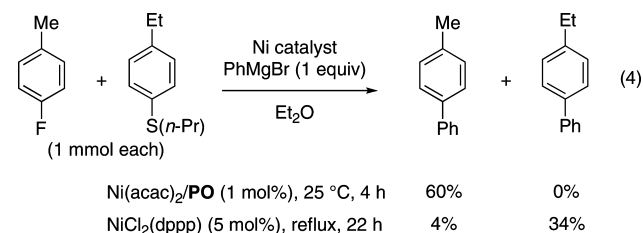
The *m*- and *p*-hydroxy analogues (**L6** and **L7**) of *o*-hydroxyphenylphosphine (**L1**) were just as ineffective as triphenylphosphine (entries 7 and 8), in agreement with the proposed proximity effect in the Ni/**L1** catalysis. The bishydroxy ligand **L8** was similarly ineffective (entry 9).

We further modified the ligand structure to suppress the formation of the homocoupling product **2**. Cyclohexanol- and benzyl alcohol-type ligands (**L9** and **L10**) effectively suppressed the byproduct formation while keeping the catalytic activity as high as that for **L1** (entries 10 and 11). The phenylethanol-type ligand **L11** (=PO, 94% yield; entry 12) showed the best performance. In contrast, the use of the tertiary alcoholic ligand **L12** resulted in a sharp drop in the catalytic activity (entry 13). The Ni/PO catalyst was reactive enough to complete the reaction with only 1 mol % catalyst loading (entry 14). The reaction was much slower in THF than in ether (entry 15). The Ni-catalyzed Negishi reaction and Pd-catalyzed KTC reaction of the aryl fluoride were not promoted by these ligands at all.

Scope and Limitation. A. Cross-Coupling with Aryl Halides, Triflate, and Sulfide. With the Ni/PO combination in hand, we studied the scope and limitation of the nickel-catalyzed KTC reaction. First, we examined the reaction of PhMgBr with conventional substrates for the nickel-catalyzed KTC reaction (Table 2). As expected, *p*-tolyl chloride was more reactive than the fluoride, and the reaction was complete within 20 min with 1 mol % catalyst (entry 2). *p*-Tolyl bromide and iodide were even more reactive and gave the cross-coupling products at

similar reaction rates with catalyst loadings of 0.2 and 0.05 mol %, respectively (entries 3 and 4). Although aryl triflates²¹ and sulfides²² are generally much more reactive than aryl fluorides in cross-coupling reactions, they were less reactive under the present conditions. The conversion of *p*-tolyl triflate was somewhat slower than that of the fluoride (entry 5). Methyl *p*-tolyl sulfide exhibited poor conversion under the same conditions (entry 6), and with 5 mol % catalyst it gave a 62% yield of the cross-coupling product (entry 7).

Competition experiments further demonstrated the utility of the present catalyst for C–F bond cleavage (eq 4):



The reaction of an equimolar mixture of 4-fluorotoluene, 1-ethyl-4-propylthiobenzene, and PhMgBr in the presence of Ni(acac)₂/PO afforded 4-methylbiphenyl (60%) and no 4-ethylbiphenyl (the aryl sulfide was entirely recovered), while the same reaction using NiCl₂(dppp) (5 mol %) gave more of the latter (34%) than the former (4%). Interestingly, the Ni/PO-catalyzed reaction was much slower in the presence of the sulfide than in its absence (Table 1, entry 1), suggesting that the sulfide group is a preferred ligand to the catalyst but does not take part in the coupling reaction.

B. Cross-Coupling with Aryl Fluorides. Table 3 shows the scope and limitation of the Ni/PO-catalyzed KTC reaction of aryl fluorides. Electron-rich and less reactive substrates bearing a 4-methoxy or 4-dimethylamino group smoothly underwent the cross-coupling reaction with PhMgBr in the presence of 1 mol % catalyst (entries 1 and 2). Electron-deficient 2-fluoropyridine gave the cross-coupling product in 96% yield with 0.2 mol % catalyst loading (entry 3). Ortho-monosubstituted aryl fluorides gave the products in 93–97% yield (entries 4–6), while ortho-disubstituted substrates such as 2-fluoro-1,3-dimethylbenzene were entirely unreactive. No sign of aryl C–O bond cleavage was observed (entries 1 and 5), though some nickel catalysts have been reported to promote KTC and other cross-coupling reactions of aryl ethers.^{7b,14} The reaction of 4-fluorostyrene was rather sluggish and gave the product in 61% yield after 48 h with 5 mol % catalyst, probably because the preferred coordination of the nickel(0) atom to the olefinic moiety retarded the C–F bond activation (entry 7).²³

The present reaction showed a significant dependence on the Grignard reagent used. While 4-methoxyphenyl- and 4-tolylmagnesium bromide reacted rapidly and cleanly (entries 8 and 9), increased steric hindrance in the Grignard reagent decelerated

- (21) (a) Hayashi, T.; Niizuma, S.; Kamikawa, T.; Suzuki, N.; Uozumi, Y. *J. Am. Chem. Soc.* **1995**, *117*, 9101–9102. (b) Kamikawa, T.; Hayashi, T. *Synlett* **1997**, 163–164. (c) Kamikawa, T.; Hayashi, T. *Tetrahedron* **1999**, *55*, 3455–3466. (d) Hayashi, T.; Ishigedani, M. *J. Am. Chem. Soc.* **2000**, *122*, 976–977. (e) Hayashi, T.; Han, J. S.; Takeda, A.; Tang, J.; Nohmi, K.; Mukaide, K.; Tsuji, H.; Uozumi, Y. *Adv. Synth. Catal.* **2001**, *343*, 279–283.
- (22) (a) Okamura, H.; Miura, M.; Takei, H. *Tetrahedron Lett.* **1979**, *20*, 43–46. (b) Wenkert, E.; Ferreira, T. W.; Michelotti, E. L. *J. Chem. Soc., Chem. Commun.* **1979**, 637–638.
- (23) Zenkina, O. V.; Karton, A.; Freeman, D.; Shimon, L. J. W.; Martin, J. M. L.; van der Boom, M. E. *Inorg. Chem.* **2008**, *47*, 5114–5121.

Table 3. Ni/**PO**-Catalyzed Cross-Coupling of Aryl Fluorides (Ar–F) and Grignard Reagents (RMgBr)^a

entry	Ar–F	R	catalyst (mol%)	time (h)	yield (%) ^b
1		Ph	1	1	93
2		Ph	1	5	87
3		Ph	0.2	2	96
4		Ph	1	5	96
5		Ph	1	9	93
6		Ph	1	1	97
7 ^c		4-MeOC ₆ H ₄	5	48	61
8 ^d		4-MeOC ₆ H ₄	2.5	12	94 (R = Me)
9		4-MeC ₆ H ₄	1	12	97 (R = OMe)
10 ^c		2-Naphthyl	5	22	72 (R = OMe)
11 ^c		1-Naphthyl	5	100	21 (R = OMe) ^e
12 ^{c,f}		2-MeC ₆ H ₄	5	48	27 (R = OMe)
13 ^{c,g}		2-MeOC ₆ H ₄	5	3	15 (R = H) ^h
14 ^{c,g}		Me	5	48	60 (R = Me) ^h

^a Unless otherwise noted, the reaction was carried out on a 1 mmol scale using 1.1 equiv of the Grignard reagent in Et₂O at 25 °C. ^b Isolated yield. ^c Using 1.5 equiv of the Grignard reagent. ^d Using 1.2 equiv of the Grignard reagent. ^e Determined by ¹H NMR using an internal standard. ^f The reaction was carried out at reflux. ^g The reaction was carried out at 60 °C in THF. ^h Determined by GC using an internal standard.

the reaction. For example, a 1-naphthyl Grignard reagent was much less reactive than a 2-naphthyl derivative (entry 11 vs entry 10). The reactions of 2-tolyl and 2-methoxyphenyl Grignard reagents were also slow (entries 12 and 13). Interestingly, the present catalytic system was ineffective for alkyl Grignard reagents. The reaction of MeMgBr was rather slow even at high temperature in THF (entry 14), and primary alkyl Grignard reagents resulted only in slow reduction of the C–F bond rather than in the expected cross-coupling.

C. Cross-Coupling of Aryl Polyfluorides and Polychlorides. The present catalysis is effective for the arylation of aromatic polyfluorides and polychlorides (Table 4). Entries 1–3 show conversion of *o*-, *m*-, and *p*-difluorobenzene into the corresponding terphenyls by the use of a nearly stoichiometric amount of PhMgBr. As expected, the reaction of *p*-difluorobenzene was the fastest, giving the product in 92% yield with 0.5 mol % catalyst loading. Triarylation of 1,3,5-trifluoro- and trichlorobenzene with 3.5 equiv of an aryl Grignard reagent took place smoothly in 88 and 91% yields, respectively (entries 4 and 5). The methoxy group in 2,4,6-trichloroanisole remained intact in the triarylation reaction (entry 6). The triphenylation of 1,2,4-trichlorobenzene was relatively slow and required refluxing conditions to achieve 89% yield (entry 7). In the

Table 4. Ni/**PO**-Catalyzed Cross-Coupling of Aromatic Polyfluorides and Polychlorides with Arylmagnesium Bromide (ArMgBr)^a

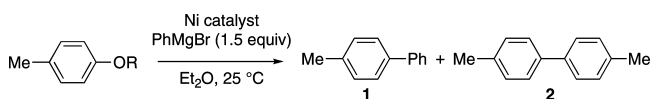
entry	substrate	Ar (equiv)	catalyst (mol%)	time (h)	product	yield (%) ^b
1		Ph (2.5)	5	48		85
2		Ph (2.1)	1	2		92
3		Ph (2.1)	0.5	1		92
4		Ph (3.5)	2.5	2		88
5		4-MeC ₆ H ₄ (3.5)	2.5	2		91
6		4-MeC ₆ H ₄ (3.5)	5	20		80
7 ^c		Ph (4.0)	5	48		89
8		4-MeC ₆ H ₄ (3.5)	5	24		85
9 ^c		Ph (5.5)	7.5	96		58

^a The reaction was carried out on a 0.5–1 mmol scale in Et₂O at 25 °C, unless otherwise noted. ^b Isolated yield. ^c The reaction was carried out at reflux.

reaction of 1,2,3-trichlorobenzene, the central C–Cl bond remained entirely intact, and a 1,3-diphenylated product was exclusively obtained in 85% yield (entry 8). Even 1,2,4,5-tetraphenylation of the corresponding tetrachloride could be achieved, albeit in a modest yield (58%; entry 9).

D. Cross-Coupling of Aryl Carbamates and Phosphates. Despite their established synthetic utility in cross-coupling with phenolic starting materials, aryl triflates are expensive and rather sensitive to hydrolysis. Therefore, reactions using less expensive and more stable alternatives, such as aryl tosylates,⁹ mesylates,¹⁰ phosphates,¹² carbamates,¹¹ carboxylates,¹³ and ethers,¹⁴ have been investigated. We thus examined the cross-coupling reactions of phenol derivatives with Grignard reagents under Ni/**PO** catalysis.

As already mentioned above, *p*-tolyl triflate reacted smoothly with PhMgBr to give the cross-coupling product **1** in 95% yield (Table 5, entry 1). Through examination of other phenol derivatives, we found that the Ni/**PO** catalyst greatly accelerated the KTC reaction of aryl phosphates and carbamates (entries 2–6). Diethyl *p*-tolyl phosphate underwent Ni/**PO**-catalyzed cross-coupling with PhMgBr as smoothly as the triflate (entry 2), while the previously reported ligand-free conditions¹² resulted in much lower conversion with the same catalyst loading (1 mol %) (entry 3). With 3 mol % loading, the Ni/**PO** catalyst smoothly promoted the KTC reaction of less reactive

Table 5. Ni-Catalyzed Cross-Coupling Reaction of *p*-Cresol Derivatives with Phenylmagnesium Bromide

entry	R	Ni catalyst	time (h)	yield (%) ^a	
				1	2
1	SO ₂ CF ₃	Ni(acac) ₂ /PO (1 mol %)	2	95	0
2	P(O)(OEt) ₂	Ni(acac) ₂ /PO (1 mol %)	2	92	0
3	P(O)(OEt) ₂	Ni(acac) ₂ (1 mol %)	2.5	9	0
4	CONEt ₂	Ni(acac) ₂ /PO (3 mol %)	1	95	4
5	CONEt ₂	Ni(acac) ₂ (5 mol %)	2.5	64	27
6	CONEt ₂	NiCl ₂ (dppp) (5 mol %)	1	10	4

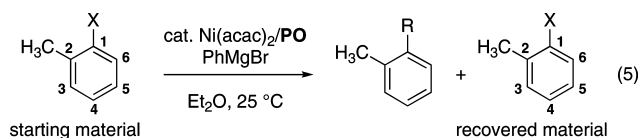
^a Determined by GC using *n*-tridecane as an internal standard.

p-tolyl diethylcarbamate (entry 4). We noted that the ligand-free conditions (5 mol %) reported by Snieckus¹¹ resulted in formation of a considerable amount of the homocoupling product **2** (entry 5). The standard nickel catalyst for the KTC reaction, NiCl₂(dppp), showed poor catalytic activity (entry 6).

The reaction of an aryl tosylate with PhMgBr exclusively resulted in homocoupling of the Grignard reagent (i.e., biphenyl formation) because the tosylate acted as an oxidant. Aryl carboxylate and carbonate esters were attacked by PhMgBr and afforded the starting phenol.

Table 6 summarizes the scope and limitation study of the Ni/PO-catalyzed KTC reaction of aryl phosphates and carbamates. Reactions with phenyl- or 4-methoxyphenylmagnesium bromide took place smoothly with para-, meta-, or ortho-monosubstituted phenyl phosphates and carbamates (entries 1–4 and 9–13), 1- and 2-naphthyl phosphates and carbamates (entries 15–18), and an estrone carbamate (entry 19) to give the desired cross-coupling products in 80–100% yields. An ortho-disubstituted carbamate showed low conversion (9% yield; entry 14). A resorcinol-derived biscarbamate gave *m*-terphenyl in 76% yield (entry 20). As we observed in the reaction of aryl fluorides, reactions of carbamates and phosphates with Ni/PO catalysis were also slowed by the steric hindrance of the Grignard reagent (entries 5–8), but not as much as in the case of the aryl fluorides (see Table 3). Thus, reactions of *o*-tolylmagnesium bromide with *p*-tolyl phosphate and carbamate gave the cross-coupling products in 50–60% yield (entries 5 and 6). Even a 2,6-dimethylphenyl Grignard reagent showed a sizable reactivity toward *p*-tolyl phosphate (entry 7).

Mechanism of Aryl-X Bond Activation. A. Kinetic Isotope Effects. To gain insight into the origin of the high activity of the Ni/PO catalyst in the KTC reaction, we measured ¹²C/¹³C kinetic isotope effects (KIEs)²⁴ in the reaction of *o*-tolyl halides (X = F, Cl, Br, I) with phenylmagnesium bromide (eq 5):



The KIE data for the catalytic reactions provide information on the first irreversible step (FIS) of the catalytic cycle, i.e., the step in which the aryl halide is irreversibly converted to a catalytic intermediate.^{19,25} If there are any elements of π

Table 6. Ni/PO-Catalyzed Cross-Coupling Reaction of Aryl Carbamates and Phosphates with Arylmagnesium Bromide (ArMgBr)^a

entry	substrate	Ar	catalyst (mol %)	time (h)	yield (%) ^b
1		Ph	1	1.5	100 (R = P(O)(OEt) ₂)
2		Ph	3	1	90 (R = CONEt ₂)
3		4-MeOC ₆ H ₄	1	13	100 (R = P(O)(OEt) ₂)
4		4-MeOC ₆ H ₄	3	1	85 (R = CONEt ₂)
5		2-MeC ₆ H ₄	5	17	54 (R = P(O)(OEt) ₂) ^c
6		2-MeC ₆ H ₄	5	7	62 (R = CONEt ₂) ^c
7		2,6-Me ₂ C ₆ H ₃	5	22	53 (R = P(O)(OEt) ₂) ^c
8		2,6-Me ₂ C ₆ H ₃	5	60	8 (R = CONEt ₂) ^c
9		Ph	3	1	96
10		4-MeOC ₆ H ₄	3	1	80
11		Ph	3	18	87
12		Ph	1	1.5	95 (R = P(O)(OEt) ₂) ^c
13		Ph	3	6	95 (R = CONEt ₂)
14		Ph	5	12	9 ^c
15		Ph	1	1	91 (R = P(O)(OEt) ₂)
16		Ph	3	1	94 (R = CONEt ₂)
17		Ph	1	1	96 (R = P(O)(OEt) ₂)
18		Ph	3	1	98 (R = CONEt ₂)
19		Ph	5	6	89
20 ^d		Ph	5	7	76

^a Unless otherwise noted, the reaction was carried out in Et₂O at 25 °C on a 0.5–1 mmol scale using 1.5 equiv of Grignard reagent. ^b Isolated yield. ^c Determined by GC using an internal standard. ^d Using 2.5 equiv of PhMgBr.

complexation in the FIS, we should observe an asymmetric distribution of KIEs over the aromatic carbon atoms. If the FIS involves C–X bond cleavage (oxidative addition), we should observe a substantial KIE at the ipso carbon atom.

Figure 1 summarizes the ¹²C/¹³C KIE data for the Ni/PO catalysis, which is shown together with data previously obtained for conventional nickel- or palladium-bisphosphine catalysis¹⁹ and the organocopper-mediated reaction.¹⁶ The Ni/PO-catalyzed reactions of *o*-tolyl fluoride, chloride, and bromide exhibited sizable KIE values at the ipso carbon atoms (C1, 1.013–1.017) and smaller values at the unsubstituted ortho carbon atoms (C6, 1.007–1.010) (Figure 1a–c). The KIE values for the rest of the aromatic ring were negligible. The data strongly suggest that the FIS of the Ni/PO catalysis involves C–X bond cleavage, where the nickel catalyst interacts with the C1–C6 moiety in an η^2 manner. The unequal distribution of the KIEs on the six carbon atoms does not favor the possibility of a single-electron-transfer mechanism in the oxidative addition, which is known for the stoichiometric reaction of an electron-rich Ni(0)–phosphine complex with an aryl iodide or bromide.²⁶ The reaction of *o*-tolyl iodide resulted in much smaller KIE values, including a positive

(24) Singleton, D. A.; Thomas, A. A. *J. Am. Chem. Soc.* **1995**, *117*, 9357–9358.

(25) Vo, L. K.; Singleton, D. A. *Org. Lett.* **2004**, *6*, 2469–2472.

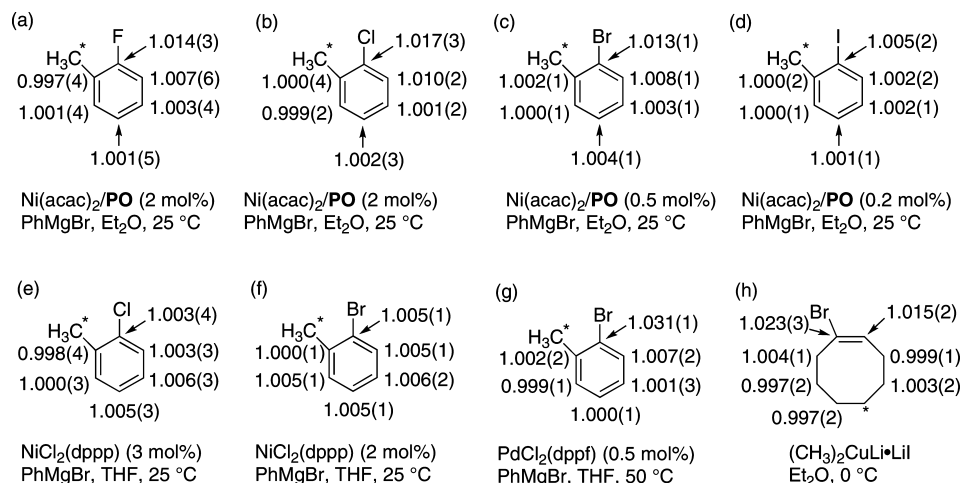
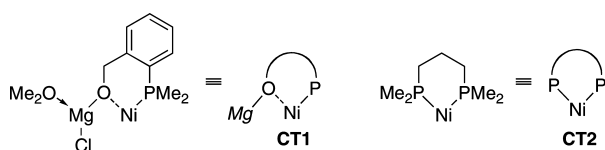


Figure 1. $^{12}\text{C}/^{13}\text{C}$ KIE values for the KTC reactions catalyzed by (a–d) $\text{Ni}(\text{acac})_2/\text{PO}$, (e, f) $\text{NiCl}_2(\text{dppp})$, and (g) $\text{PdCl}_2(\text{dppf})$ and for (h) an organocopper-mediated substitution reaction. The asterisked carbon atom was taken as a reference for each KIE measurement (KIE = 1 was assumed). Data in (e–g) and (h) were taken from refs 19 and 16, respectively.

Chart 2. Model Ni Complexes Used in the Theoretical Study



KIE at C1 (1.005) (Figure 1d), suggesting that C–I bond cleavage takes place through a very early transition state.

The KIE data for the Ni/PO catalysis (Figure 1a–c) are in stark contrast to those for the conventional Ni–bisphosphine catalysis (Figure 1e,f)¹⁹ but show a trend similar to those for the case of the Pd–bisphosphine catalysis (Figure 1g)¹⁹ and the organocopper-mediated reaction (Figure 1h).¹⁶ Those previ-

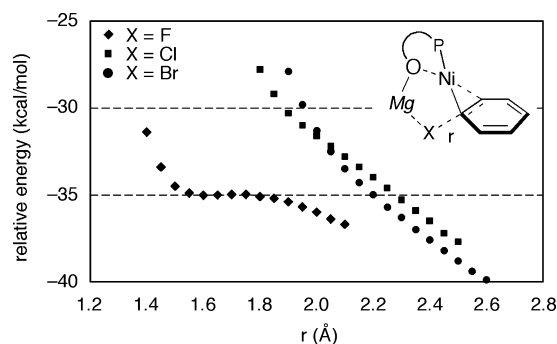


Figure 2. Change in potential energy of the CT1–halobenzene complex (shown in the upper-right corner) with elongation of the C–X bond length r .

Scheme 1. Reaction of Ni/Mg Bimetallic Species CT1 and Halobenzene PhX (X = F, Cl, Br)

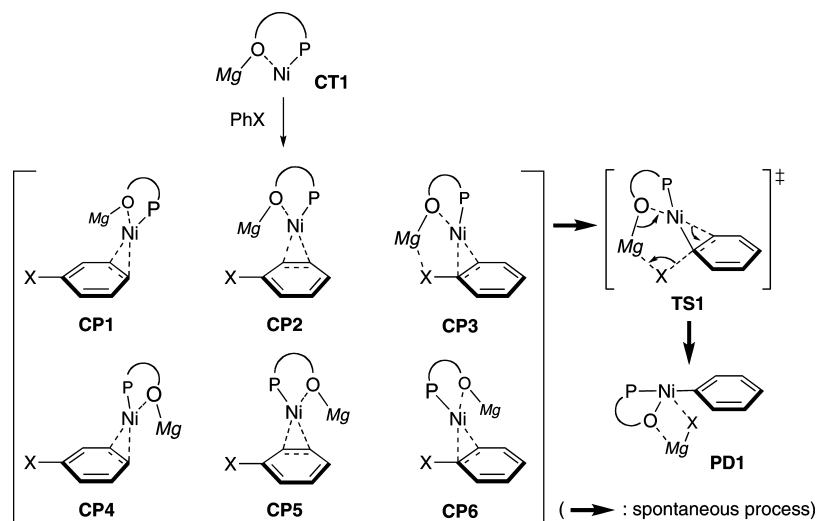
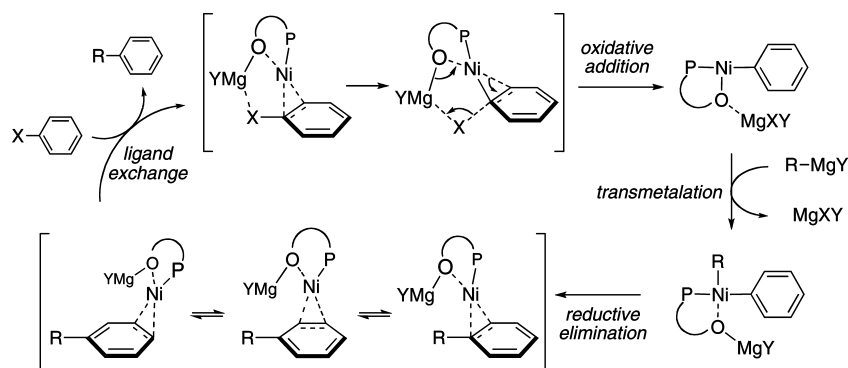


Table 7. Relative Potential Energies and Gibbs Free Energies (kcal/mol) of Ni/Mg Complexes in Scheme 1^a

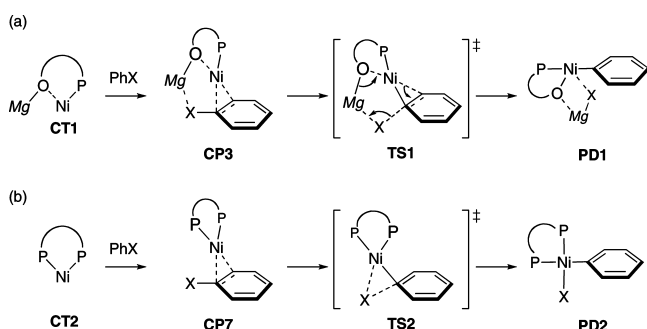
X	CP1	CP2	CP3	CP4	CP5	CP6	TS1	PD1
F	–24.4 (–13.0)	–33.3 (–20.7)	N/A ^b	–25.0 (–13.9)	–30.6 (–17.7)	–27.6 (–15.5)	N/A ^b	–52.8 (–40.8)
Cl	–24.8 (–13.0)	–27.1 (–14.3)	N/A ^b	–25.8 (–13.9)	–28.7 (–16.7)	–30.3 (–17.6)	N/A ^b	–54.0 (–41.7)
Br	–25.0 (–13.0)	–27.9 (–15.3)	N/A ^b	–26.0 (–14.3)	–28.8	–32.1 (–19.2)	N/A ^b	–56.2 (–44.0)

^a Calculated at the B3LYP level using LANL2DZ for Ni, Ahlrichs SVP for Br, and 6-31G(d) for the rest. Gibbs free energies are shown in parentheses. ^b The structures could not be located because of spontaneous C–X bond cleavage during the geometry optimization (see Figure 2).

Scheme 2



Scheme 3. Oxidative Addition of a Phenyl Electrophile [X = OP(O)(OMe)₂, OCONMe₂, OMe, SMe] to Nickel Complexes (a) **CT1** and (b) **CT2**



ous data indicated that the FIS of the Ni–bisphosphine catalysis is the coordination of the Ni catalyst on the less hindered side of the π face of the substrate, while the FIS of the Pd catalysis or the Cu reaction corresponds to the C–X bond cleavage step, where the metal atom interacts with the substrate in an η^2 manner.

B. DFT Study of the Aryl–X Bond Activation Step. To gain a better understanding of the experimental KIE data, we performed density functional theory (DFT) calculations on the interaction of a model catalytic species with fluorobenzene, chlorobenzene, or bromobenzene.²⁷ We chose the nickel phosphine/magnesium alkoxide bimetallic complex **CT1** as a model catalytic species, where the ligand **PO** acts as an anionic P,O-bidentate ligand for nickel upon deprotonation by the Grignard reagent (Chart 2).

The catalyst **CT1** was allowed to interact with a halobenzene PhX (X = F, Cl, Br) in all six possible orientations. Five of these possibilities resulted in the formation of η^2 complexes **CP1**, **CP2**, and **CP4–CP6** (Scheme 1) with large stabilization energies ranging from 24.4 to 33.0 kcal/mol (Table 7), which are comparable to the stabilization energy for complexation of **CT1** with benzene (26.9 kcal/mol). However, the one remaining possibility, the putative η^2 complex **CP3**, decomposed without an activation barrier to give arylnickel(II) complex **PD1**. What is special about **CP3** is the bimetallic binding to the halogen atom and the ipso/ortho C–C bond.

To gain insight into the nature of the putative complex **CP3**, we performed geometry optimizations for a variety of fixed C–X (X = F, Cl, Br) bond lengths; these indicated that the potential surface for the C–X bond cleavage is very flat (X = F) or simply downhill (X = Cl, Br) (Figure 2). The formation of **PD1** from **CT1** and the halobenzene is highly exothermic ($\Delta E = -53$ to -56 kcal/mol). This spontaneous bond cleavage process attests to the validity of our bimetallic synergy, as illustrated by a hypothetical transition state **TS1**.

The behavior of the Ni/Mg complex **CT1** is in strong contrast to that of a nickel–bisphosphine complex such as **CT2** (Chart 2), which shows no particular regiochemical preference in the η^2 complexation with an aryl halide or related species and undergoes oxidative addition through a three-centered-insertion TS, as previously reported by us and others.^{19,23,28–30}

The above result indicates that a nickel/magnesium species such as **CT1** shows a strong preference for the dual interaction with an aryl halide. Thus, once the nickel and magnesium atoms approach the ipso/ortho position and the halogen atom, respectively, back-donation by Ni(0) and Lewis acid activation by Mg(II) cooperatively promote the C–X bond cleavage in a push–pull manner. This mechanistic picture is schematically illustrated in Scheme 2 and is qualitatively consistent with the KIE data for the Ni/PO catalysis (Figure 1a–c). The absence of the C–X bond cleavage TS (**TS1**) on the potential surface did not allow theoretical evaluation of the KIE values and quantitative comparison with the experimental results (it should be noted that the present theoretical calculations do not provide information on the free-energy surface, which should be uphill because of the entropy cost of the bimolecular association).

Some characteristics of the Ni/PO catalytic system deserve further theoretical analysis, namely, (1) the high reactivity toward aryl phosphates and carbamates (Tables 5 and 6), (2) the inertness of the aryl–OMe bond (entries 1 and 5 in Table 2), and (3) the low reactivity toward an aryl sulfide (entries 6 and 7 in Table 2; eq 4). Thus, we briefly studied the reactions of **CT1** with dimethyl phenyl phosphate, phenyl dimethylcarbamate, anisole, and thioanisole (Scheme 3a). For these unreactive substrates, an η^2 complex (**CP3**) and C–X bond cleavage TS (**TS1**) could be located. For comparison, the reaction of the nickel–bisphosphine complex **CT2** was also examined (Scheme 3b). In this case, the reaction goes through an η^2 complex **CP7**

(26) (a) Tsou, T. T.; Kochi, J. K. *J. Am. Chem. Soc.* **1979**, *101*, 6319–6332. (b) Tsou, T. T.; Kochi, J. K. *J. Am. Chem. Soc.* **1979**, *101*, 7547–7560.

(27) The DFT calculations were performed at the B3LYP level using the LANL2DZ basis set for Ni, the Ahlrichs SVP basis set for Br, and the 6-31G(d) basis set for the rest of the atoms. See the Supporting Information for details of the computational methods.

(28) Atesin, T. A.; Li, T.; Lachaize, S.; García, J. J.; Jones, W. D. *Organometallics* **2008**, *27*, 3811–3817.

(29) Reinhold, M.; McGrady, J. E.; Perutz, R. N. *J. Am. Chem. Soc.* **2004**, *126*, 5268–5276.

(30) Schaub, T.; Fischer, P.; Steffen, A.; Braun, T.; Radius, U.; Mix, A. *J. Am. Chem. Soc.* **2008**, *130*, 9304–9317.

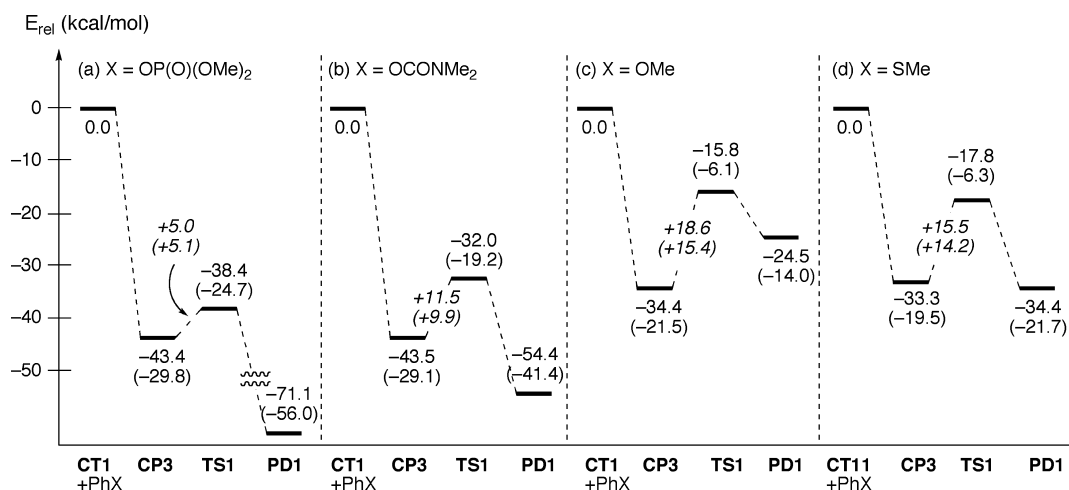


Figure 3. Potential energy diagrams for the reaction of **CT1** and (a) dimethyl phenyl phosphate, (b) phenyl dimethylcarbamate, (c) anisole, and (d) thioanisole. Gibbs free energies are indicated in parentheses.

and a three-centered oxidative addition TS (**TS2**) and gives arylnickel complex **PD2**.

The energy profiles for the reactions of **CT1** are shown in Figure 3. The catalyst **CT1** shows a much stronger interaction with the phosphate and the carbamate to form **CP3** ($\Delta E \approx -43$ kcal/mol) than with anisole and thioanisole ($\Delta E \approx -34$ kcal/mol). This is probably due to a strong Lewis acid/Lewis base interaction between the Mg atom and the P=O or C=O oxygen atom (see Figure 4a,b). The activation energy for the C–X bond cleavage (i.e., from **CP3** to **TS1**) is lowest for the phosphate ($\Delta E^\ddagger = 5.0$ kcal/mol). The carbamate reaction takes place with an activation energy as low as 11.5 kcal/mol, while much higher activation energies are needed for anisole (18.6 kcal/mol) and thioanisole (15.5 kcal/mol). The trend in the activation energy parallels the structure of the oxidative-addition TS: the reaction of the phosphate goes through a much earlier TS than those of the carbamate and anisole, as characterized by the C–O and Ni–C2 bond lengths (Figure 4). The conversion of the η^2 complex **CP3** to the arylnickel complex **PD1** is highly exothermic for the phosphate and the carbamate, while it is endothermic for anisole and almost thermoneutral for thioanisole. These computational data are qualitatively consistent with the experimental observations, in particular, the facile cross-coupling reactions of aryl phosphates and carbamates as well as the reluctance of aryl ethers and sulfides to take part in the reaction.

Analysis of the reactions of the nickel–bisphosphine complex **CT2** with the phenol derivatives or thioanisole gave energy profiles (Figure 5) that are quite different from those of **CT1** (Figure 3), which corroborates the unique reactivity of the bimetallic complex **CT1**. Thus, the stabilization energies for the η^2 complexes **CP7** formed between **CT2** and the phenol derivatives (i.e., phosphate, carbamate, and anisole) are very close to each other ($\Delta E = -13.9$ to -17.0 kcal/mol; Figure 5a–c). Furthermore, the oxidative addition of the phenol derivatives (**CP3** to **TS2**) requires rather high activation energies of similar magnitude (21.6 to 25.3 kcal/mol), whereas the exothermicity of the reaction is much larger for the phosphate and the carbamate than for the anisole. In addition, the reaction of thioanisole is characterized by a larger η^2 complexation energy (-20.9 kcal/mol) and a much lower activation energy (12.6 kcal/mol) than for the reaction of the phenol derivatives (Figure 5d).

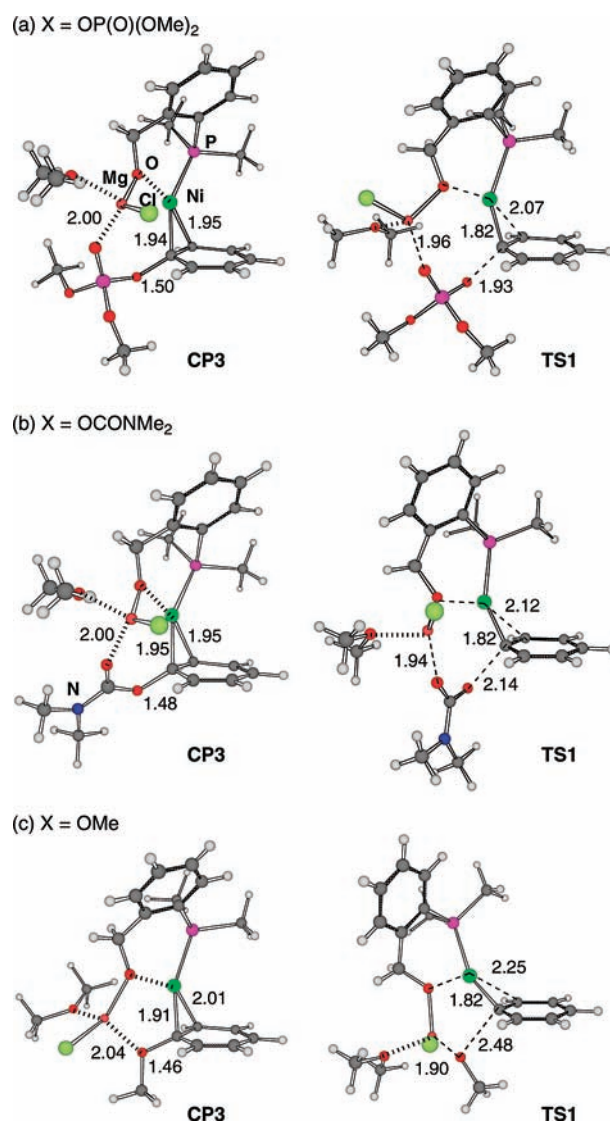


Figure 4. Structures of η^2 complexes and oxidative-addition TSs in the reactions of **CT1** with phenyl electrophiles [X = OP(O)(OMe)₂, OCONMe₂, OMe]. Color code: gray, carbon; white, hydrogen; green, nickel; red, oxygen; pink, phosphorus; blue, nitrogen; light-green, chlorine; orange, magnesium.

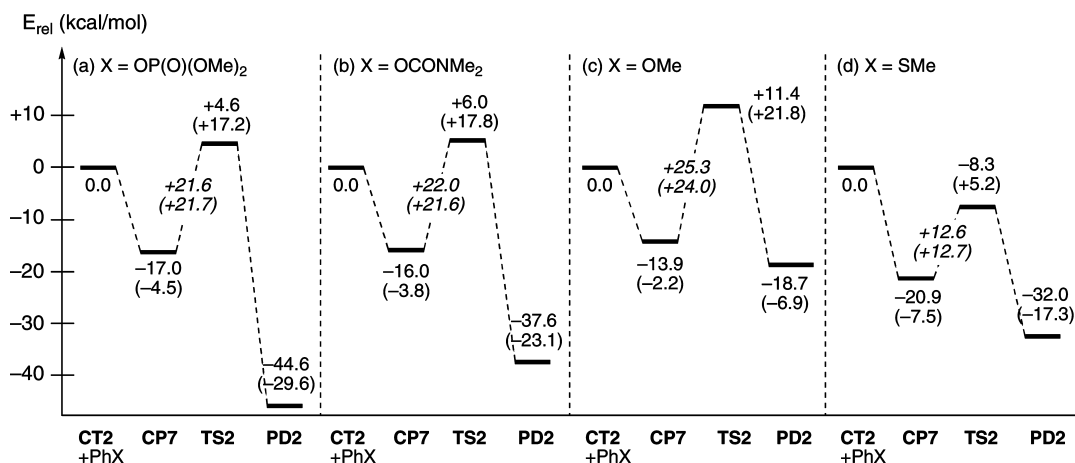


Figure 5. Potential energy diagrams for the reaction of CT2 and (a) dimethyl phenyl phosphate, (b) phenyl dimethylcarbamate, (c) anisole, and (d) thioanisole. Gibbs free energies are indicated in parentheses.

Chart 3. Rationalization of the Reactivities of CT1 and CT2 toward Phenol Derivatives and Thioanisole [X = P(OMe)₂, CNMe₂]

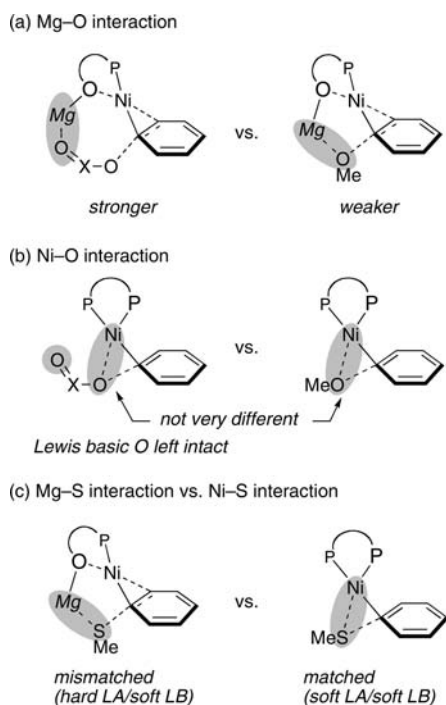
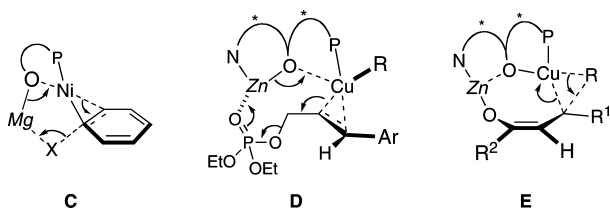


Chart 4. Cooperative Effects of the Transition Metal and Lewis Acid Organized by PO and PON Ligands



The characteristic reactivity difference between CT1 and CT2 can be illustrated schematically as shown in Chart 3. First, the Ni/Mg complex CT1 shows a much higher reactivity toward the phosphate and the carbamate than toward the anisole because it enjoys a stronger Mg–leaving-group interaction during the C–O bond cleavage as a result of the much higher Lewis basicity of the P=O or C=O oxygen atom than of the methoxy

oxygen atom (Chart 3a). On the other hand, the reactivities of CT2 toward the phosphate, carbamate, and anisole are not very much different, because these reactions go through similar three-centered TSs in which the Lewis basic oxygen atoms of the phosphate and the carbamate are left intact (Chart 3b). Finally, the bimetallic activation by CT1 does not work very well for thioanisole because of the mismatched Lewis acid/Lewis base interaction between the hard Mg atom and the soft S atom, whereas the three-centered TS of CT2 benefits from the matched interaction between the soft Ni atom and the soft S atom (Chart 3c).¹⁷

Conclusion

We have reported in this paper that hydroxyphosphine ligands (PO ligands) greatly accelerate the nickel-catalyzed cross-coupling reaction of unreactive aryl electrophiles and Grignard reagents. Thus, the reaction can utilize unreactive aryl halides such as fluorides, chlorides, polyfluorides, and polychlorides as well as phenol derivatives such as carbamates and phosphates. Experiments and theory have indicated that the nickel(II) precatalyst, the PO ligand, and the Grignard reagent form a nickel/magnesium bimetallic catalytic species through reduction of Ni(II) to Ni(0) and deprotonation of the PO ligand and that this catalytic species then carries out push–pull, cooperative activation of the aryl electrophile via the nucleophilic nickel and the Lewis acidic magnesium centers (C in Chart 4). Similar cooperative mechanisms account for the high level of stereochemical control of copper-catalyzed C–C bond-formation reactions by chiral PON ligands (eqs 2 and 3).²⁰ Thus, the nucleophilic copper and Lewis acidic zinc centers assembled on the deprotonated form of the PON ligand cooperatively activate an allylic electrophile (D in Chart 4) or an enone (E in Chart 4) in a stereoselective manner. In summary, the present work not only provides a practically useful catalyst for the cross-coupling reaction but also offers a rationale for tailor-designed bimetallic catalysts for cooperative, chemoselective, and stereoselective activation of electrophilic substrates.³¹

(31) (a) *Multimetallic Catalysts in Organic Synthesis*; Shibasaki, M., Yamamoto, Y., Eds.; Wiley-VCH: Weinheim, Germany, 2004. (b) Shibasaki, M.; Matsunaga, S.; Kumagai, N. *Synlett* **2008**, 1583–1602. (c) Matsunaga, S.; Shibasaki, M. *Bull. Chem. Soc. Jpn.* **2008**, *81*, 60–75.

Acknowledgment. We thank MEXT/JSPS for financial support [KAKENHI 18105004 (S) to E.N., 20037012 (Chemistry of Concerto Catalysis) to N.Y., and the Global COE program for Chemistry Innovation]. The generous amount of computational time from the Research Center for Computational Science, Okazaki National Research Institute, is gratefully acknowledged.

Supporting Information Available: Experimental procedures, characterization of new compounds, computational methods, and Cartesian coordinates of stationary points. This material is available free of charge via the Internet at <http://pubs.acs.org>.

JA903091G